Water-assisted mobile charge induced screening and origin of hysteresis in carbon nanotube field-effect transistors

Y. Pascal-Levy,[1,2] E. Shifman,[2] M. Pal-Chowdhury,[2] I. Kalifa,[2] T. Rabkin,[1,2] O. Shtempluck,[2] A. Razin,[2]
V. Kochetkov,[2] and Y. E. Yaish[2,*]

[1]*Russell Berrie Nanotechnology Institute, Technion, Haifa 32000, Israel*
[2]*Department of Electrical Engineering, Technion, Haifa 32000, Israel*

Carbon nanotube field-effect transistors (CNT FETs) have many possible applications in future nanoelectronics due to their excellent properties. However, one of the major challenges regarding their performance is the noticeable gate hysteresis which is often displayed in their transfer characteristics. The hysteresis phenomenon is often attributed to water-mediated charge transfer between the CNT and the dielectric layer or the CNT and the water layer itself. In this study, we implement the usage of current versus time measurements in addition to the traditional transfer characteristics to accurately extract the time constants of the hysteresis of suspended and on-surface CNT FETs. Following a thorough study, we provide experimental evidence that the hysteresis phenomenon of suspended CNT FETs, as well as of on-surface CNT FETs which operate at low gate voltage regimes ($|V_g| < 3$ V), is based on gate-induced, water-assisted redistribution of mobile charge on the SiO_2 surface, and is not related to charge injection from the CNT itself. Our model is confirmed by an electronic-force-microscopy-based measurement technique which enables us to quantify the temporal surface charge distribution while measuring CNT currents.

I. INTRODUCTION

Due to their excellent performance and high sensitivity to many kinds of analytes, single-wall carbon nanotube field-effect transistors (CNT FETs) have been the subject of many studies that focus mainly on device applications. Yet several unresolved issues need to be clarified before further successful utilization of these devices can take place. One of these issues is the noticeable gate hysteresis that CNT FETs usually exhibit in their transfer characteristics. This phenomenon has previously been explained by several different models. Mobile charges or ions that can be relocated within the dielectric layer by sweeping the gate voltage are known from silicon metal-oxide semiconductor (MOS) FETs to cause retarded hysteresis;[1] however, CNT FETs usually exhibit advanced hysteresis, which indicates that this mechanism is not the main reason for this phenomenon. Defects in the CNT itself could function as charging centers with the applied gate voltage and cause hysteresis;[2–4] nonetheless, it has been shown that the amount of hysteresis of CNT FETs can be controlled by the design of the gate dielectric, indicating that defects in the CNT are a minor contributor.[5] The high electric field could cause a rearrangement of adsorbents on the CNT which act as dopants;[6] however, it is difficult to explain the significant shift of the threshold voltage—usually from positive to negative—simply through rearrangement of electron acceptors.

In light of this, gate hysteresis has usually been attributed to stationary charge traps within the dielectric, which are filled and emptied by the applied gate voltage with charge transfer to and from the CNT itself.[7–11] These findings suggest that CNTs behave like leaky FETs where charges can flow back and forth between the CNT and the surface, and that the total tube charge is changing with time. However, later on, the hysteresis phenomenon was observed for suspended CNTs as well.[12] It has been shown that water molecules that adhere to the

surface of the CNT give a large contribution to the hysteresis, and therefore it has been suggested that the hysteresis is due to a water layer which is bound to the surface of the CNT, and behaves as a charge trap or a mediator.[12–14] Nonetheless, this explanation raises several difficulties. The possibility of water molecules acting as charge traps has been questioned,[15,16] as has their role as mediators, since ionic charge transfer mediated by water should theoretically cause a retarding hysteresis.

As mentioned, the common explanation for the hysteresis which is driven by water molecules is based on electric charges that have been added to or removed from the CNT while sweeping the gate, and as a result have modified the current. A simple model for this behavior, which assumes a linear relation between the depleted charges and the total current, is based on a resistor-capacitor (RC) circuit where the tube is presented by a leaky capacitor with resistance R.[17] However, the current through the CNT does not depend linearly on the tube total charge, and a more accurate statement is that the current depends on the electric potential along the CNT, φ, using the transfer characteristic, i.e., $I = f(\varphi)$. For example, charges that have been accumulated near the CNT can modify φ, and as a result the total current will be modified respectively. In this paper, we introduce an RC model as well, but we suggest that for suspended CNT FETs, as well as for on-surface CNT FETs which operate at low gate potentials ($|V_g| < 3$ V), the resistance as well as capacitance elements arise mainly from the oxide itself and not from leakage current to or from the CNT.

Bradley *et al.*[18] have controllably introduced hysteresis by coating CNT FETs with charged polymers, and they proposed that the effect results from ionic motion. However, experimental evidence was scarce, and the mechanism of the process remained unknown. Below, we present an extensive study of hysteresis in suspended CNTs, and we argue that mobile charges are indeed relevant. Using a method to

calculate the accurate time constants of the hysteresis, we provide experimental evidence that the hysteresis is caused by water-assisted movement of mobile charges on the SiO_2 surface. This movement, which aims to bring the system to a lower energetic configuration, is a direct result of the gate bias. Furthermore, we provide evidence that the above-mentioned mechanism underlies the hysteresis phenomenon in on-surface CNT FETs as well for low gate operational biases. Our model is examined using a technique which implements the usage of electrostatic force microscopy (EFM) to gain quantitative information on the substrate lateral and temporal charge distribution, CNT currents, and hysteresis time constants, and the results support our hypothesis.

II. EXPERIMENTS

Suspended CNT FETs were fabricated using a growth-at-the-end method[19,20] in order to avoid any additional sources for the hysteretic phenomenon from residual process contamination. The processing was performed on 1 μm/500 nm SiO_2 thermally grown on highly *p*-doped silicon substrate using photolithography techniques. First, the source and drain were patterned with 5/40 nm chrome/platinum electrodes, with gaps of 1.3/1.8 μm between them. Next, the devices were submerged in 1:6 buffer oxide etch (BOE) for two minutes in order to etch trenches about 200 nm deep between each electrode pair. Finally, iron nanoparticles were deposited at specific places on top of the electrodes, and the CNTs were grown by chemical vapor deposition (CVD) with a methane/hydrogen gas mixture at 900 °C. This technique yields extremely clean devices, since the CNT growth is performed at the last step of the process, and all resist residues are burned and disposed of in the CVD process. To create on-surface CNT FETs, suspended devices were submerged in

deionized water for a couple of seconds and then allowed to dry in ambient air for several hours. Figures 1(a) and 1(c) show a schematic and a scanning electron microscope (SEM) image of a suspended CNT FET, respectively. Figures 1(b) and 1(d) show a schematic and a SEM image of an on-surface CNT FET, respectively. In SEM images, on-surface CNTs appear significantly brighter and thicker than the suspended ones.[21] Figure 1(e) is an atomic force microscopy (AFM) picture of an on-surface CNT FET. The smooth and clean surface is very noticeable.

III. RESULTS AND DISCUSSION

When suspended CNT FETs were exposed to an ambient environment, hysteresis was observed in the current (I_{ds}) versus gate voltage (V_g) characteristics when V_g was swept between -3 and 3 V [see Fig. 3(a)]. The hysteresis was advancing in nature, and its width (which is defined as the difference in the threshold gate voltages between the down and the up sweep directions) exhibited a strong dependence on ambient humidity, as was previously reported.[13,22] The

FIG. 2. (Color online) (a) The hysteresis width of a suspended CNT exhibiting an exponential dependence on the gate scanning time with time constant $\tau = 38 \pm 4.2$ s. V_g is swept between -3 and 3 V, and $V_{ds} = 10$ mV. Error bars are smaller than the markers. (b) I_{ds} (blue) as a function of time for the same CNT as in (a) while applying a series of gate voltages: 0, -3, 0, 3, and 0 V. This series repeats itself three times (green). Inset: zoom-in into single current decay curve, I_{ds} time, following compliance of $V_g = -3$ V and exponential fit (red) to it.
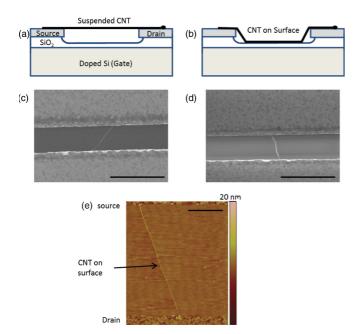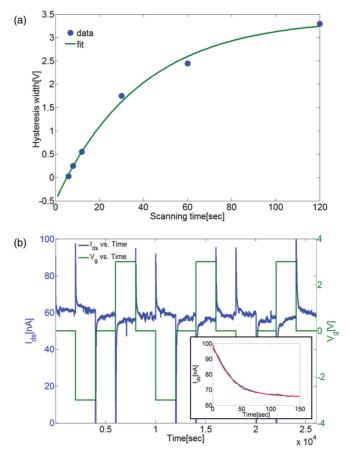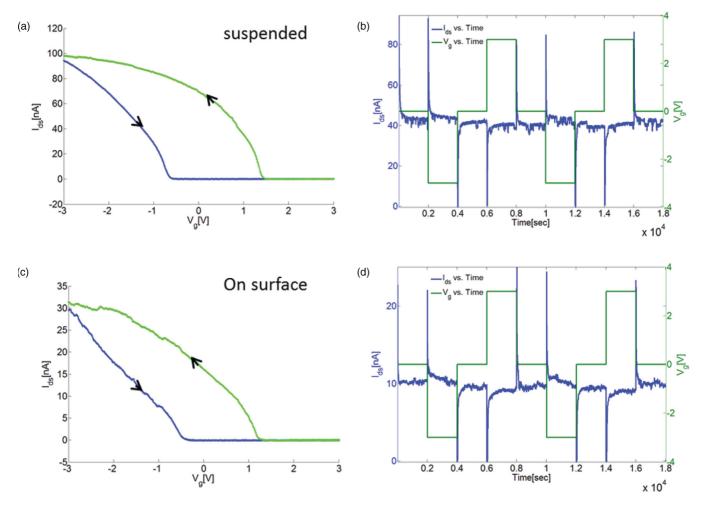
FIG. 1. (Color online) (a) A schematic of a suspended CNT. (b) A schematic of an on-surface CNT. (c) A SEM image of a suspended CNT. (d) A SEM image of an on-surface CNT. (e) An AFM image of an on-surface CNT. All the scale bars are 4 μm.

FIG. 3. (Color online) (a) I_{ds}-V_g of a suspended CNT FET. Scan rate is 200 mV/s, and $V_{ds} = 10$ mV. (b) I_{ds} (blue) as a function of time for the same CNT as in (a) while applying a series of values to V_g: 0, -3, 0, 3, and 0 V. This series repeats itself twice (green). (c) I_{ds}-V_g of the same CNT FET as in (a) after the CNT was adhered to the surface. Scan rate and V_{ds} are the same as before. (d) I_{ds} (blue) as a function of time for the same CNT as in (c) while applying a series of values to V_g: 0, -3, 0, 3, and 0 V. This series repeats itself twice (green).

hysteresis width has also exhibited an exponential time dependence on the scanning time of a single sweep period with a time constant of $\tau = 38 \pm 4.2$ s [see Fig. 2(a)]. This dependence, which is in agreement with earlier observations of hysteresis in CNT FETs,[18] suggests that the hysteresis is caused by a slow-moving species-carrying charge.

Based on this evidence, we implemented the usage of a more accurate measurement aimed at extracting the time constants of the hysteresis effect. As shown in Fig. 2(b), we measured I_{ds} as a function of time while applying a series of gate voltages: 0, -3, 0, 3, and 0 V. This series of values repeated itself several times. Two main findings were observed: (a) the data can be divided into two pairs of gate voltages, $V_g = 0$ and 3 V ($V_g = -3$ and 0 V), on which the current shows a rapid decrease (increase) followed by a slow recovery (decay); (b) after a long time during which the gate voltage was kept constant, the currents for all the gate voltages tended to the same value. Moreover, for each value of V_g that was kept constant for a fixed period of time, I_{ds} had converged back to its initial value exponentially. The time constants of I_{ds} for each value of V_g were extracted by fitting the data to an exponential function [see the inset in Fig. 2(b)], and an average time constant of

$\tau_{av} = 35.3 \pm 8.5$ s was found. This τ_{av} agrees reasonably well with the time constant which was extracted from Fig. 2(a), with a relative error of 8.4%. This suggests that sweeping the gate voltage with different speeds, or measuring the current versus time for a fixed gate voltage, results in the same hysteresis phenomenon, and we will utilize both methods in order to clarify its origin.

To determine whether suspended and on-surface CNT FETs exhibit similar hysteretic and time constant behavior, we examined the hysteresis phenomena of the same suspended and on-surface CNT FET. Figures 3(a) and 3(b) depict I_{ds}-V_g and I_{ds}-time measurements for a typical suspended device; an average $\tau_{av} = 19.5 \pm 6.3$ s was found according to the method discussed before. Afterward, the device was submerged in deionized water in order to make the CNT adhere to the surface (as was verified by AFM), dried for several hours, and the hysteresis was examined again [see Figs. 3(c) and 3(d)]. This time an average $\tau_{av} = 19.07 \pm 5.3$ s was deduced. One can observe that I_{ds} was reduced roughly by third after the CNT touched the surface, and the device became somewhat noisier; however, the hysteretic characteristics did not change and the time constants remained nearly the same, with a relative error
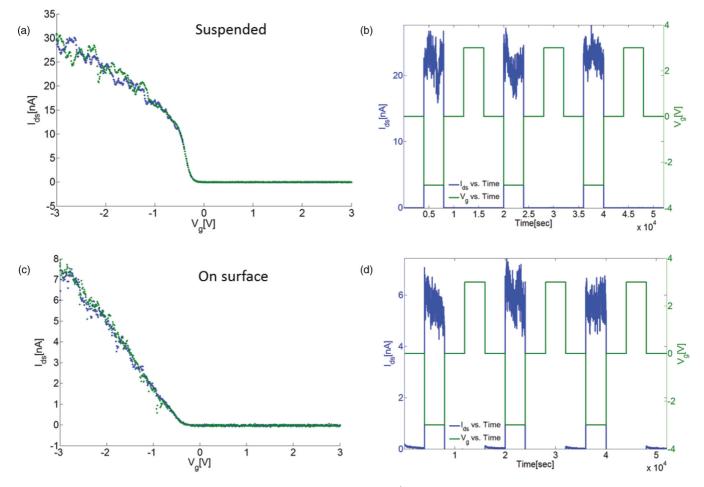
FIG. 4. (Color online) (a) I_{ds}-V_g of a suspended CNT FET in vacuum ($\sim 10^{-6}$ torr). Scan rate is 200 mV/s, and $V_{ds} = 10$ mV. (b) I_{ds} (blue) as a function of time for the same CNT in (a), while applying a series of gate voltages: 0, -3, 0, 3, and 0 V. This series repeats itself three times (green). (c) I_{ds}-V_g of an on-surface CNT FET in vacuum ($\sim 10^{-6}$ torr). Scan rate and V_{ds} are as before. (d) I_{ds} (blue) as a function of time for the same CNT as in (c) while applying a series of gate voltages: 0, -3, 0, 3, and 0 V. This series repeats itself three times (green).

of 2.2%. The same behavior was found for five other tubes as well. These results suggest that the same mechanism underlies the hysteresis phenomenon in both types of CNT FETs for small V_g sweep ranges.

Next, we conducted a series of control experiments in order to unveil the mechanism that is responsible for the hysteresis in these CNTs. As shown in Figs. 4(a) and 4(c), upon changing the environment for suspended and on-surface CNT FETs from ambient air to vacuum ($\sim 10^{-6}$ torr), the hysteresis reduced to near zero almost immediately, indicating its strong dependence on one or several components of the air. As was expected, the I_{ds} time measurements changed as well [Figs. 4(b) and 4(d)]: upon changing V_g, I_{ds} immediately changed accordingly, but then remained constant and did not converge exponentially back to its initial value, as was found previously at ambient conditions. For higher values of V_g in vacuum, the behavior of the two types of CNT FETs differs: in suspended CNTs, the hysteresis does not reappear at all (up to $V_g = \pm 10$ V); however, for on-surface CNTs, the hysteresis begins to reappear only above ~ 4 V. This observation indicates that additional mechanisms exist for on-surface CNT FETs which are contributing to the hysteresis phenomenon at higher gate voltages. One possible mechanism is charge injection

from the tube itself, as was suggested previously,[7] and it should indeed depend on the gate voltage, either for field emission processes or thermally assisted tunneling. However, for the rest of this study, we restrict our measurements and analysis to small gate voltages for on-surface CNTs.

Exposing the CNTs to different atmospheres may provide clues about which ingredients are essential for the hysteresis phenomenon. Figure 5 depicts the results of introducing several atmospheres which are abundant in ambient air while sweeping V_g continuously between -3 and 3 V. As has already been mentioned, the hysteresis disappeared almost entirely upon changing the environment from ambient air to vacuum [Fig. 5(a)]. Also, the current reduced significantly, probably due to the removal of oxygen, which is known to modulate the Schottky barriers and alter the p-channel current.[23] We found that the hysteresis did not reappear upon exposure to oxygen [Fig. 5(b)], nor upon exposure to nitrogen [Fig. 5(c)]. However, when water vapors were introduced into the cell, the hysteresis gradually increased once again [Fig. 5(d)]. This observation is consistent with previous findings, which have reported that humidity affects hysteresis significantly.[12,13,22]

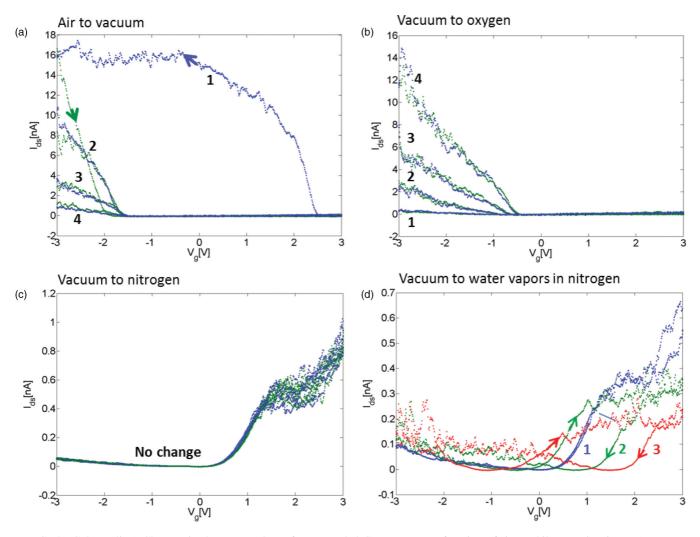The same hysteretic behavior and atmospheric dependence were found for small band gap CNTs as well. These are

FIG. 5. (Color online) Changes in the I_{ds}-V_g plots of a suspended CNT FET as a function of time while exposing it to (a) vacuum, (b) oxygen, (c) nitrogen, and (d) water vapors. The scan rate in all the plots is 200 mV/s and $V_{ds} = 10$ mV.

metallic CNTs with a small band gap that is usually formed as a consequence of tube deformation.[24,25] One can utilize these metallic tubes in order to find the location of the water layer on the device. For that purpose, we continuously measured I_{ds} versus V_g for a suspended, metallic CNT FET [see Fig. 6(a)], while increasing the bias voltage V_{ds} gradually at the end of each sweep. The width of the hysteresis for each sweep is shown in the inset of Fig. 6(b) as a function of V_{ds}. Previously, it has been shown that under high source-drain biases, suspended metallic CNTs are heated to several hundred degrees centigrade, since the heat dissipates mainly through the metallic contacts and the surrounding air, which is a poor thermal conductor.[26] A signature for such heat-enhanced phonon scattering is typically observed in the negative differential conductance at high V_{ds}, as found for our device as well (see Fig. 7). At such elevated temperatures, any water layer that might be adhered to the tube surface would probably evaporate and disappear. Nonetheless, the hysteresis did not decrease and remained nearly constant throughout the experiment [inset of Fig. 6(b)]. However, when the same CNT FET was placed on a hot plate and its I_{ds} versus V_g characteristics were continuously recorded while the hot plate

temperature gradually increased (V_g was swept between -3 and 3 V, and V_{ds} was kept constant at 10 mV), the results were completely different. Figure 6(b) shows the width of the hysteresis that was obtained in each sweep as a function of the hot plate temperature. In this case, the hysteresis is rapidly reduced and reaches near zero at about 35 °C. This process was carried out on more than 10 suspended metallic and semiconducting CNTs, and they all showed the same hysteresis behavior versus source-drain bias, V_{ds}, and hot plate temperature.

These results suggest that contrary to common belief, hysteresis is caused by water molecules that adhere to the oxide and not to the CNT itself. However, since our experiments were conducted using CNTs which were suspended relatively far above the SiO$_2$ surface on which the water molecules were located, charge transfer between the water layer and the CNT became impossible. Thus, the water layer cannot function as a charge trap or mediator for charge transfer between the CNT and the oxide, as was previously believed.[12–14] Furthermore, because on-surface CNTs exhibit similar hysteretic behavior with roughly the same time constants as suspended CNTs for low operational gate voltages ($|V_g| < 3$ V), we argue that for
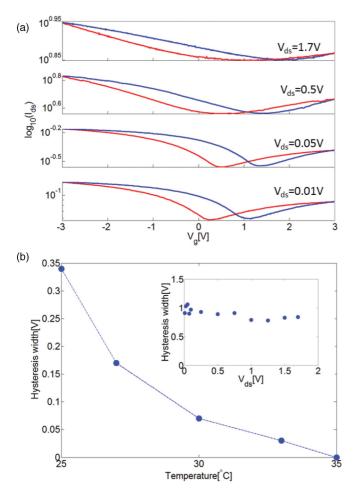
FIG. 6. (Color online) (a) Semilog plots of I_{ds}-V_g of a suspended, metallic CNT for several values of V_{ds}. In all of these curves, the scan rate was 200 mV/s. (b) Hysteresis width for the same CNT as in (a) as a function of the hot plate temperature. $V_{ds} = 10$ mV, and V_g is swept between -3 and 3 V with a scan rate of 200 mV/s. Inset: hysteresis width for the same CNT as in (a) as a function of V_{ds}. Error bars are smaller than the markers.

these conditions, charge injection is not the dominant cause of hysteresis of on-surface CNTs as well.
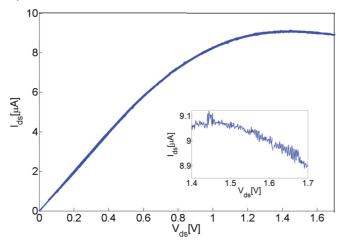

FIG. 7. (Color online) I_{ds}-V_{ds} of the same suspended metallic CNT as in Fig. 6. Inset: Zoom-in at high V_{ds}, where negative differential conductance due to heat-enhanced phonon scattering is observed.
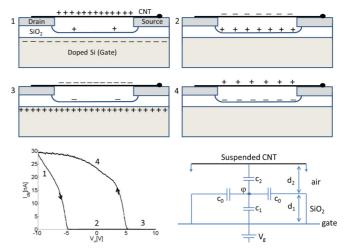

FIG. 8. (Color online) A schematic of the gate-screening process. In state 1, V_g is negative and therefore induces positive charge on the CNT, resulting in high conductance. Meanwhile, positive charge starts assembling on the SiO$_2$ surface, gradually screening the gate. In state 2, V_g becomes zero. However, the positive charge which has assembled on the SiO$_2$ surface during state 1 cannot react quickly and induces negative charge on the CNT, thus the CNT conductance is zero. In state 3, V_g is positive and is pushing the CNT Fermi level deep into its band gap where no current is allowed. Negative charge is beginning to assemble on the SiO$_2$ surface. In state 4, V_g is back to zero again. However, the negative charge which has assembled on the SiO$_2$ surface during state 3 induces positive charge on the CNT, and the conductance is finite and higher than in state 2, resulting in a hysteresis loop. Bottom right: an equivalent circuit for the hysteresis model. C_1 and C_2 are the oxide and air capacitors, respectively. C_0 is the surface leaky capacitor where charge redistribution is taking place.

We propose that water-assisted mobility of surface charge on the SiO$_2$ surface is the underlying mechanism for the hysteresis phenomenon observed in suspended CNTs for all V_g regimes (up to ± 10 V) and for on-surface CNTs for low gate voltages (up to ± 3 V). A schematic of the gate-screening process involving mobile charges on the SiO$_2$ surface is given in Fig. 8. As a nonzero value of V_g is applied, opposite-signed mobile charge drifts across the SiO$_2$ surface through the water layer and gradually screens the gate electric field from the CNT. The movement of the charges results in a lower energetic configuration of the electric field lines. A rough estimation of the electrostatic energy for a CNT-gate capacitor configuration including the gate battery is given by $E_{\text{CNT}} = -CV^2/2 = -\pi\varepsilon_0\varepsilon_{\text{ox}}LV^2/\ln(\frac{2d}{R}) \approx -98$ eV, where L is the length of the CNT ($\simeq 1$ μm), R is its diameter ($\simeq 1$ nm), d is the oxide thickness ($\simeq 500$ nm), and $V = 1$ V. On the other hand, for a simple plate capacitor configuration in the same approximate effective area, the energy is $E_{\text{PC}} = -CV^2/2 = -A\varepsilon_0\varepsilon_{\text{ox}}V^2/2d = -215$ eV, where A is taken to be $2dL$. This model also explains the observations of I_{ds} versus time which are presented in Figs. 2(b), 3(b), and 3(d); when V_g is changed to a certain nonzero value and then kept constant, I_{ds} changes immediately accordingly. However, the charge that is continuously assembled on the SiO$_2$ surface gradually screens V_g from the CNT, eventually causing I_{ds} to converge to its initial value, equal to the value obtained at $V_g = 0$ V. In Figs. 4(b) and 4(d), on the other hand, the device is under
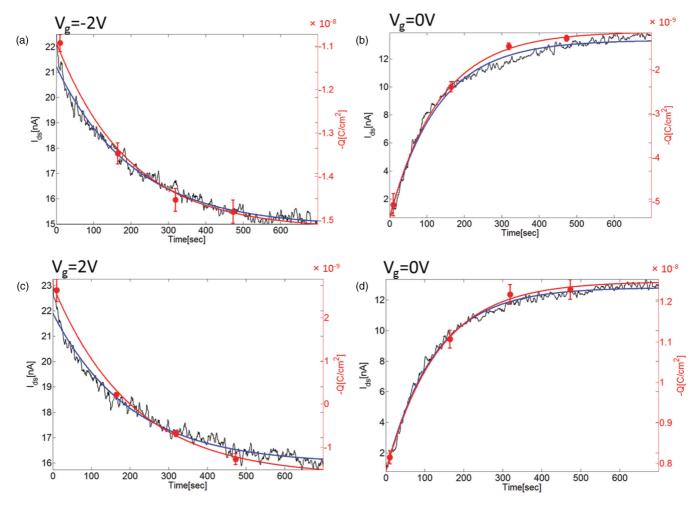
FIG. 9. (Color online) EFM-based measurements of the temporal charge distribution on the SiO_2 surface in close proximity to an on-surface CNT (red circles). Red lines are best fit to exponential behavior. Simultaneously, I_{ds} vs time was measured (black lines) with a bias voltage of 10 mV. Blue lines are best fit to exponential time dependence. The measurements were conducted for four values of V_g: (a) $V_g = -2$ V, (b) $V_g = 0$ V, (c) $V_g = 2$ V, and (d) $V_g = 0$ V.

deep vacuum, thus the absence of a water layer prevents the charge from drifting across the SiO_2 surface, and therefore I_{ds} remains constant and does not change with time.

In a recent study,[27] we reported on gate-induced water-assisted surface charge redistribution on dielectric layers. Briefly, the temporal behavior for this phenomenon indeed follows an exponential time dependence which was attributed to charge transport along the oxide surface that acts as a leaky capacitor. The time constants for this behavior are long, and are inversely dependent on the oxide conductivity. The charge movement is a consequence of drift current under lateral electric fields that originate from the back gate external compliance. We have argued that this surface conductivity depends strongly on humidity, but the exact microscopic physical mechanism underlying this dependence is still unclear and requires further studies.

An equivalent simplified circuit for the system can be composed from the following elements, as depicted in the bottom right of Fig. 8. As has already been mentioned, the electric potential along the CNT, V_{CNT}, is not identical to V_g due to the capacitances of the SiO_2 (C_1; see Fig. 8, bottom right) and the air (C_2), and due to the capacitance of the mobile

ions on the SiO_2 surface (C_0). This potential can be expressed as $V_{CNT} \approx \varphi$, where φ is given by $\frac{(C_1 + 2C_0)V_g}{C_2 + C_1 + 2C_0}$. According to this expression, for small values of d_2, C_2 will be significant, and the expression for φ will become $\frac{(C_1 + 2C_0)V_g}{C_2}$, resulting in a pronounced hysteresis. On the other hand, for big enough values of d_2, C_2 will become very small, and φ will tend to V_g, resulting in a very small hysteresis. Experiments we have conducted for suspended CNTs with deeper trenches indeed show smaller hysteresis, in agreement with previous study.[28]

To examine this model, we used a technique[27] which employs the use of EFM to gain quantitative information on the substrate charge distribution. Using this technique, we measured the amount of charge in close proximity to an on-surface CNT as a function of time while measuring the CNT's current under the following gate voltage compliances: 0, −2, 0, 2, and 0 V. The results are shown in Fig. 9. The surface charge density declines (inclines) in an exponential decay (recovery) manner which is very similar to that of I_{ds}, with equivalent time constants for all V_g regimes (maximum relative error 8.5%). Moreover, the amount of total charge that moves on the substrate during the measurement is roughly the same for all gate voltages [$(4.2 \times 10^{-9}) \pm (0.2 \times 10^{-9})$ C/cm^2],

and its sign in each regime matches the expected one (see Fig. 8). Far from the tube ($\sim20\ \mu$m), a similar behavior is observed with similar time constants, which confirms that charge transport on the oxide surface has nothing to do with the leakage current to or from the tube itself. Note that for the CNT in Fig. 9, there is a variance in the time constants of the declining currents ($\tau \approx 200$ s) and the time constants of the inclining currents ($\tau \approx 130$ s). This variance was observed with varying relative errors for suspended CNTs as well, and we speculate that this observation has to do with the different mobilities of positive and negative charges which are strongly influenced by surface contamination. However, the exact origin for this difference is still unclear, and further studies are needed to clarify it.

IV. CONCLUSIONS

In conclusion, in the current study we have conducted a thorough investigation of the origin of hysteresis of suspended and on-surface CNTs. Using I_{ds}-time measurements in addition to the prevalent I_{ds} versus V_g characteristics measurements, we were able to extract the accurate time constants of the hysteresis phenomenon. To find out which component of the ambient environment is responsible for the effect, we conducted a series of control experiments which confirmed that humidity is the major cause of hysteresis. However, we found that the location of the water layer is on the SiO_2 surface rather than on the CNT itself. On the basis of these results, it was concluded that water-assisted mobility of charge on the SiO_2 surface is the underlying mechanism for the hysteresis phenomenon in suspended CNTs. By comparing the time constants of suspended CNTs with the time constants of on-surface CNTs in which the CNTs were adhered to the surface, we proved that the above-mentioned mechanism is also responsible for the hysteresis of on-surface CNTs operating at low gate voltages ($|V_g| < 3$ V). At higher gate values, additional mechanisms start to contribute to the hysteresis phenomenon of on-surface CNTs, and are the subject of further studies. A model for the hysteresis involving surface charge redistribution aimed to screen the applied gate voltage was proposed and supported by quantitative temporal EFM charge distribution measurements. This model explains not only the temporal dependence of the screening phenomenon, but also the final steady-state value of the current for any gate voltage which is found regularly for these devices.

These findings are of fundamental importance not only to CNT devices, but also to nanoscale devices in general, as they may help to control or completely eliminate the hysteresis phenomenon seen in those devices as well. Moreover, various sensing mechanisms that were suggested for nanoscale devices on top of insulating substrates should be reconsidered regarding our results. We argue that different analytes that modify the transfer characteristic of nanodevices may alter the insulating substrates' conductivity, and as a result may affect the device conductance. This possibility paves the way to much more sensitive detectors that are sensitive to the substrates' conductivity and not merely to their own sensing area.

*yuvaly@ee.technion.ac.il

[1] K. Vanheusden, W. L. Warren, R. A. B. Devine, D. M. Fleetwood, J. R. Schwank, M. R. Shaneyfelt, P. S. Winokur, and Z. J. Lemnios, Nature (London) **386**, 587 (1997).

[2] M. Freitag, A. T. Johnson, S. V. Kalinin, and D. A. Bonnell, Phys. Rev. Lett. **89**, 216801 (2002).

[3] J.-Y. Park, Appl. Phys. Lett. **90**, 023112 (2007).

[4] Y. Kim, Y. M. Oh, J.-Y. Park, and S.-J. Kahng, Nanotechnology **18**, 475712 (2007).

[5] M. Rinkio, A. Johansson, M. Y. Zavodchikova, J. J. Toppari, A. G. Nasibulin, E. I. Kauppinen, and P. Torma, New J. Phys. **10**, 103019 (2008).

[6] H. Lin and S. Tiwari, Appl. Phys. Lett. **89**, 073507 (2006).

[7] M. S. Fuhrer, B. M. Kim, T. Drkop, and T. Brintlinger, Nano Lett. **2**, 755 (2002).

[8] M. Radosavljevic, M. Freitag, K. V. Thadani, and A. T. Johnson, Nano Lett. **2**, 761 (2002).

[9] A. Vijayaraghavan, S. Kar, C. Soldano, S. Talapatra, O. Nalamasu, and P. M. Ajayan, Appl. Phys. Lett. **89**, 162108 (2006).

[10] D. Estrada, S. Dutta, A. Liao, and E. Pop, Nanotechnology **21**, 085702 (2010).

[11] A. Robert-Peillard and S. Rotkin, Nanotechnology: IEEE Trans. **4**, 284 (2005).

[12] W. Kim, A. Javey, O. Vermesh, Q. Wang, Y. Li, and H. Dai, Nano Lett. **3**, 193 (2003).

[13] P. S. Na, H. Kim, H.-M. So, K.-J. Kong, H. Chang, B. H. Ryu, Y. Choi, J.-O. Lee, B.-K. Kim, J.-J. Kim, and J. Kim, Appl. Phys. Lett. **87**, 093101 (2005).

[14] R. Pati, Y. Zhang, S. K. Nayak, and P. M. Ajayan, Appl. Phys. Lett. **81**, 2638 (2002).

[15] D. Sung, S. Hong, Y.-H. Kim, N. Park, S. Kim, S. L. Maeng, and K.-C. Kim, Appl. Phys. Lett. **89**, 243110 (2006).

[16] J. S. Lee, S. Ryu, K. Yoo, I. S. Choi, W. S. Yun, and J. Kim, J. Phys. Chem. C **111**, 12504 (2007).

[17] S. Kar, A. Vijayaraghavan, C. Soldano, S. Talapatra, R. Vajtai, O. Nalamasu, and P. M. Ajayan, Appl. Phys. Lett. **89**, 132118 (2006).

[18] K. Bradley, J. Cumings, A. Star, J.-C. P. Gabriel, and G. Grner, Nano Lett. **3**, 639 (2003).

[19] J. Cao, Q. Wang, M. Rolandi, and H. Dai, Phys. Rev. Lett. **93**, 216803 (2004).

[20] J. Cao, Q. Wang, D. Wang, and H. Dai, Small **1**, 138 (2005).

[21] T. Brintlinger, Y.-F. Chen, T. Durkop, E. Cobas, M. S. Fuhrer, J. D. Barry, and J. Melngailis, Appl. Phys. Lett. **81**, 2454 (2002).

[22]M. Rinkio, M. Y. Zavodchikova, P. Torma, and A. Johansson, Phys. Status Solidi B **245**, 2315 (2008).

[23]V. Derycke, R. Martel, J. Appenzeller, and P. Avouris, Nano Lett. **1**, 453 (2001).

[24]E. D. Minot, Y. Yaish, V. Sazonova, J.-Y. Park, M. Brink, and P. L. McEuen, Phys. Rev. Lett. **90**, 156401 (2003).

[25]J. Cao, Q. Wang, and H. Dai, Phys. Rev. Lett. **90**, 157601 (2003).

[26]E. Pop, D. Mann, J. Cao, Q. Wang, K. Goodson, and H. Dai, Phys. Rev. Lett. **95**, 155505 (2005).

[27]Y. Pascal-Levy, E. Shifman, I. Sivan, I. Kalifa, M. Pal-Chowdhury, O. Shtempluk, A. Razin, V. Kochetkov, and Y. E. Yaish (unpublished).

[28]M. Muoth, T. Helbling, L. Durrer, S.-W. Lee, C. Roman, and C. Hierold, Nat. Nanotech. **5**, 589 (2010).